JOURNAL OF MATERIALS SCIENCE 36 (2001) 4181–4188

Phase transformation behavior and wire drawing properties of Ti-Ni-Mo shape memory alloys

TAE-HYUN NAM, DAE-WON CHUNG, JUNG-PIL NOH, HEE-WOO LEE
Division of Materials Science and Engineering, Gyeongsang National University & RIIT, 900 Gazwa-dong, Chinju, Gyeong Nam 660-701, Korea
E-mail: tahynam@nongae.gsnu.ac.kr

Transformation behavior and wire drawing properties of Ti-Ni-Mo shape memory alloys have been investigated by means of differential scanning calorimetry (DSC) measurements, X-ray diffraction, electron microscopy, tensile tests and wire drawing tests. Mo addition to a Ti-Ni binary alloy induced the R phase transformation, and consequently Ti-Ni-Mo alloys showed two stage transformation, i.e., from the B2(cubic) parent phase to the R(rhombohedral) phase, and then from the R phase to B19′(monoclinic) phase. In the thermo-mechanically treated 51Ti-48.3Ni-0.7Mo alloy, reverse transformation temperature, Af, kept constant, irrespective of thermo-mechanical treatment conditions, while it changed in the thermo-mechanically treated 51Ti-49Ni and 51Ti-48.5Ni-0.5Mo alloys. Mo addition to Ti-Ni binary alloy decreased wire drawing stress. Wire drawing stress decreased with raising intermediate annealing temperature monotonously when the annealing treatment was made in vacuum. When the annealing treatment was made in air, however, it decreased with raising annealing temperature up to 923 K, and then increased. Optimum intermediate annealing temperature of Ti-Ni-Mo alloys for wire drawing was 823 K, above which a thick oxide film which reduced the drawability of the alloys was formed on the surface of alloy wires.

1. Introduction

Near equiatomic Ti-Ni alloy is the most attractive one among many shape memory alloys from practical points of view because of its superior shape memory effect, pseudoelasticity and ductility. Many applications of Ti-Ni alloys for actuators and medical instruments have been made, in which Ti-Ni alloys are usually deformed to wire form. Ti-Ni alloys are known to be tensile deformed to more than 50% strain prior to fracture, but their large strain hardening hinders their workability [1]. In order to avoid fracturing during wire drawing, an intermediate annealing to release internal stress introduced by cold drawing is necessary. Therefore, commercial manufacturing process of Ti-Ni wires involves repeated cold drawing and subsequent annealing.

Cold working and subsequent annealing, thermo-mechanical treatment, has been known to improve the shape memory effect and pseudoelasticity of Ti-Ni alloys because it increased the critical stress for slip deformation of the alloys [2, 3]. Also thermo-mechanical treatment has been known to affect transformation temperatures and behavior in the alloys. Fully annealed near equiatomic Ti-Ni alloys transforms in one stage, i.e., from the B2(cubic) parent phase to the B19′(monoclinic) martensitic phase, while some thermo-mechanically treated alloys transforms in two stages, i.e., from the B2 to R(rhombohedral), and then from the R to B19′ [4, 5].

Wu *et al*. reported that thermo-mechanical treatment conditions, i.e., amount of cold working, annealing temperature and annealing time, affect largely the wire drawing properties of Ti-Ni binary alloys [6]. According to them, the drawing stress decreases with decreasing the amount of cold working and with increasing annealing temperature. Also they pointed out that high temperature annealing over 973 K was detrimental to the pseudoelasticity because of the thick oxide film formed on the surface of the wire [6].

Ti-Ni-Mo shape memory alloys are very attractive because of their good corrosion resistance. According to Gunter [7], the corrosion resistance of Ti-Ni-Mo alloys is much better than pure Ti which is widely used as an implant material in medical field and Ti-Ni-Mo alloys are of great promise for medical applications. For medical applications such as staples, clamps and stent [8], Ti-Ni-Mo alloys should be manufactured to wire. Transformation behavior and drawing properties of Ti-Ni-Mo alloys, however, have not been reported yet. In the present study, we aimed to investigate the transformation behavior and wire drawing properties of Ti-Ni-Mo shape memory alloys. Also results obtained are compared with those obtained from Ti-Ni binary alloys.

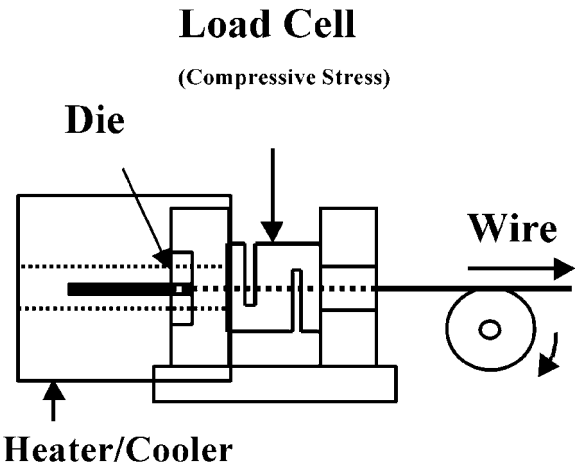

Figure 1 Apparatus for measuring the drawing stress.

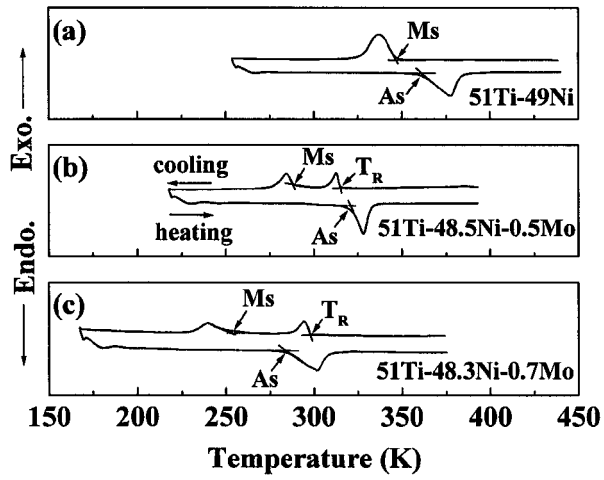

Figure 2 DSC curves of the fully annealed (a) 51Ti-49Ni, (b) 51Ti-48.5Ni-0.5Mo and (c) 51Ti-48.3Ni-0.7Mo alloys.

2. Experimental procedure

51Ti-49Ni, 51Ti-48.5Ni-0.5Mo and 51Ti-48.3Ni-0.7Mo(at%) alloy ingots were prepared by vacuum induction in a graphite crucible. After the alloy ingots being hot rolled into rods, specimens for wire drawing (Φ 3.0 mm × 200 mm) were cut from the rods. All specimens were fully annealed at 1123 K for 3.6 ks in vacuum. The drawing machine is shown in Fig. 1. The machine is equipped with heating/cooling facilities and a load cell for measuring drawing force. The wire drawing were carried out under the speed of 5 m/min at various temperatures using drawing dies of tungsten carbide. The multi-pass wire drawing were made. The multiple-pass means that the set cross-section area reduction is achieved by continuously passing through many dies. For multi-pass drawing, intermediate annealings were done at 623 K–1123 K for 0.6 ks–3.6 ks. For eliminating the effect of oxide film on the drawing force, intermediate annealing treatments were undertaken in vacuum.

In order to investigate the transformation behavior, transformation temperatures, deformation characteristics of Ti-Ni and Ti-Ni-Mo alloy wires, differential scanning calorimetry (DSC), X-ray diffraction, transmission electron microscopy (TEM) and tensile tests were carried out. DSC measurements were carried out with heating and cooling speed of 10 K/s. X-ray diffractions were made in a temperature range of 373 K and 223 K using Cu K_α. Tensile tests were carried out at room temperature with strain rate of 2.7×10^{-4}/s. TEM observations were made with a JEM-2010 operated at 200 kV.

3. Results and discussion

3.1. Phase transformation behavior of Ti-Ni-Mo alloys

Fig. 2 shows DSC curves of fully annealed 51Ti-49Ni, 51Ti-48.5Ni-0.5Mo and 51Ti-48.3Ni-0.7Mo alloys. In the 51Ti-49Ni alloy, one clear peak appears on each cooling and heating curve as seen in Fig. 2a. In the Ti-Ni-Mo alloys, however, two peaks separated clearly on cooling curves in both alloys appear, although only one peak appears on heating curves as seen in Fig. 2b and c. In order to explain the DSC peaks, X-ray diffractions were carried out, and then results obtained are shown in Fig. 3. In the diffraction pattern of (a) obtained at

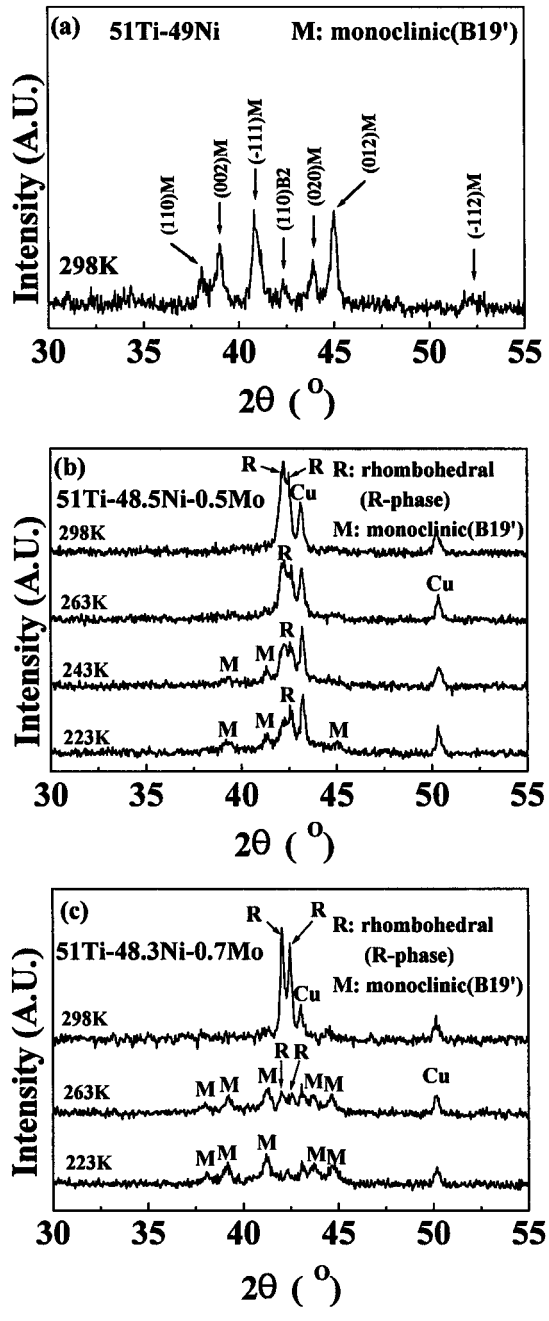

Figure 3 X-ray diffraction patterns of the fully annealed (a) 51Ti-49Ni, (b) 51Ti-48.5Ni-0.5Mo and (c) 51Ti-48.3Ni-0.7Mo alloys.

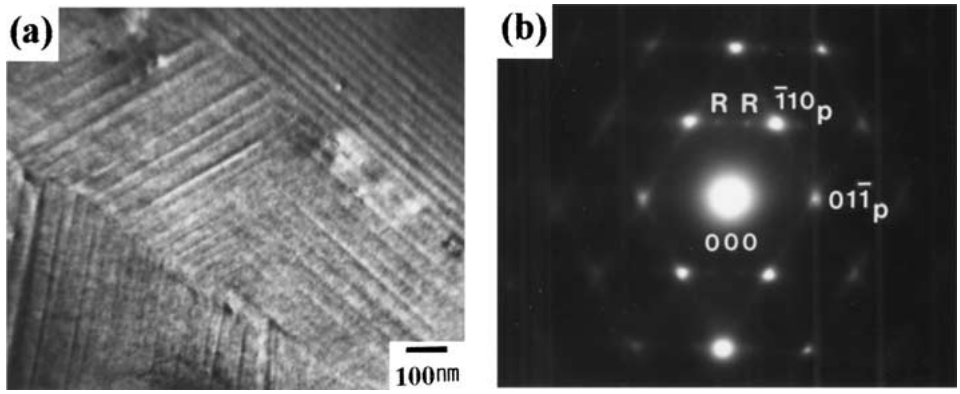

Figure 4 TEM micrographs of the fully annealed 51Ti-48.3Ni-0.7Mo alloy.

room temperature, diffraction peaks corresponding to the B19′ martensitic phase are seen. Therefore, the DSC peaks in Fig. 2a is known to be due to the B2-B19′ transformation. In the diffraction patterns of (b) and (c), diffraction peaks corresponding to the R phase are seen in the pattern obtained at 298 K. The diffraction peaks designated by Cu are due to sample holder. On cooling the specimen, intensity of the R phase diffraction peaks decreases, while that of the B19′ martensite increases. The two peaks appeared in cooling curves of Fig. 2b and c, therefore, are ascribed to the B2-R and the R-B19′ transformations, respectively.

Fig. 4 shows transmission electron micrographs of the 51Ti-48.3Ni-0.7Mo alloy. Fig. 4a is a bright field image where 3 kinds of the R phase variants are seen and (b) is an electron diffraction pattern which is a typical pattern of the R phase. From Figs 2–4, it is concluded that Mo addition to Ti-Ni alloy induces the R phase, and that transform occurs in two stages on cooling, i.e., the B2-R, and then R-B19′. Fe [9, 10] and Al [11] addition to Ti-Ni alloys have been known to induce the R phase also.

Figs 5–7 show typical DSC curves of thermo-mechanically treated 51Ti-49Ni binary and 51Ti-48.5Ni-0.5Mo and 51Ti-48.3Ni-0.7Mo ternary alloys, respectively. Annealing temperatures and times are designated on the curves. In the 51Ti-49Ni alloy, two peaks

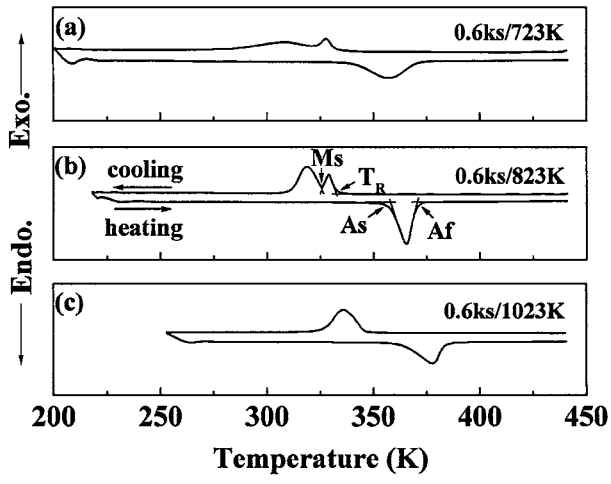

Figure 5 DSC curves of the thermo-mechanically treated 51Ti-49Ni alloy.

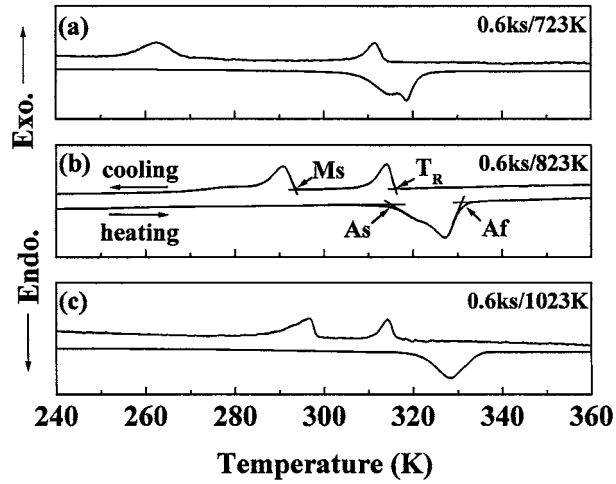

Figure 6 DSC curves of the thermo-mechanically treated 51Ti-48.5Ni-0.5Mo alloy.

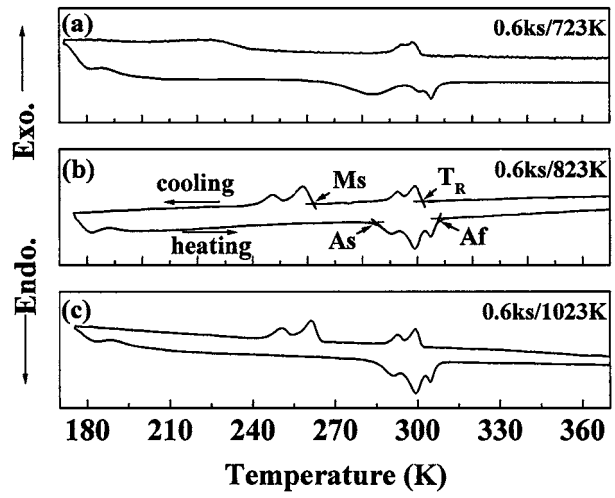

Figure 7 DSC curves of the thermo-mechanically treated 51Ti-48.3Ni-0.7Mo alloy.

appear on cooling curves when annealing temperatures are below 823 K, while only one peak appears at 1023 K as seen in Fig. 5. On heating curves only one peak appears, irrespective of annealing temperatures. In the 51Ti-48.5Ni-0.5Mo alloy, two peaks appear on cooling curves, irrespective of annealing temperatures, as seen in Fig. 6. On heating curves, two peaks appear when annealing temperatures are below 823 K, while

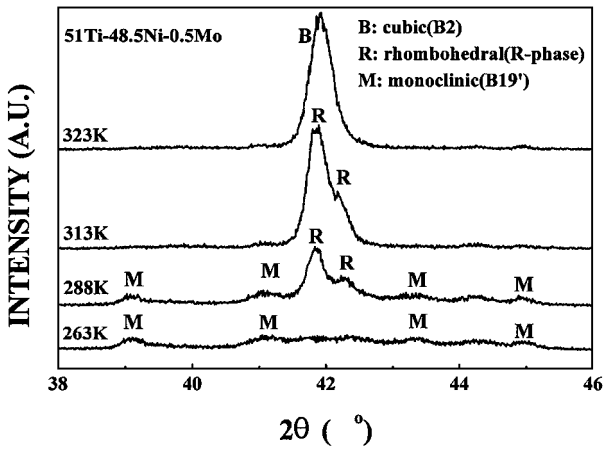

Figure 8 X-ray diffraction patterns of the thermo-mechanically treated 51Ti-48.5Ni-0.5Mo.

only one peak appears at 1023 K. In the 51Ti-48.3Ni-0.7Mo, four peaks appear on cooling curves when annealing temperatures are above 823 K, while two broad peaks appear at 623 K as seen in Fig. 6. On heating curves, three peaks appear, irrespective of annealing temperatures.

In order to explain the DSC peaks in Fig. 6b, X-ray diffraction experiments have been made, and then results obtained are shown in Fig. 8. At 323 K, only a diffraction peak corresponding to (110)B2 is seen. On cooling, diffraction peaks of the R phase appear at 313 K. On further cooling, diffraction peaks of the R and the B19′ phase appear simultaneously at 288 K. With decreasing temperature from 288 K to 263 K, intensity of peaks of the R phase decreases, whereas that of the B19′ increases. Therefore, the DSC peak at higher temperature on the cooling curve in Fig. 6b is known to be due to the B2-R transformation and that at lower temperature is to the R-B19′ transformation. From the previous study [12], transformation behavior of thermo-mechanically treated 51Ti-49Ni and 51Ti-48.3Ni-0.7Mo alloys was known to be from the B2 to R, and then from the R to the B19′. In the 0.7Mo alloy annealed at 823 K and 1023 K, DSC peaks corresponding to the B2-R and R-B19′ splits into two peaks, respectively.

Transformation temperatures of T_R(the R phase transformation start temperature), Ms (the B19′ phase transformation start temperature), As (the reverse transformation start temperature) and Af (the reverse transformation finish temperature) of thermo-mechanically treated 51Ti-49Ni, 51Ti-48.5Ni-0.5Mo and 51Ti-48.3Ni-0.7Mo are measured on DSC curves, and then plotted against annealing temperatures in Fig. 9. Changes in T_R are seen to be very small with raising annealing temperature, while those in Ms and As to be large. Similar results have been reported in Ti-Ni alloys [5]. It is to be noted here that Af increases in the 51Ti-49Ni and 51Ti-48.5Ni-0.5Mo alloys with raising annealing temperatures, whereas it keeps constant at about 310 K which is the temperature of human body in the 51Ti-48.3Ni-0.7Mo alloy. This is ascribed to the fact that the B19′-R and the R-B2 reverse transformations are not separated clearly in the 51Ti-49Ni and

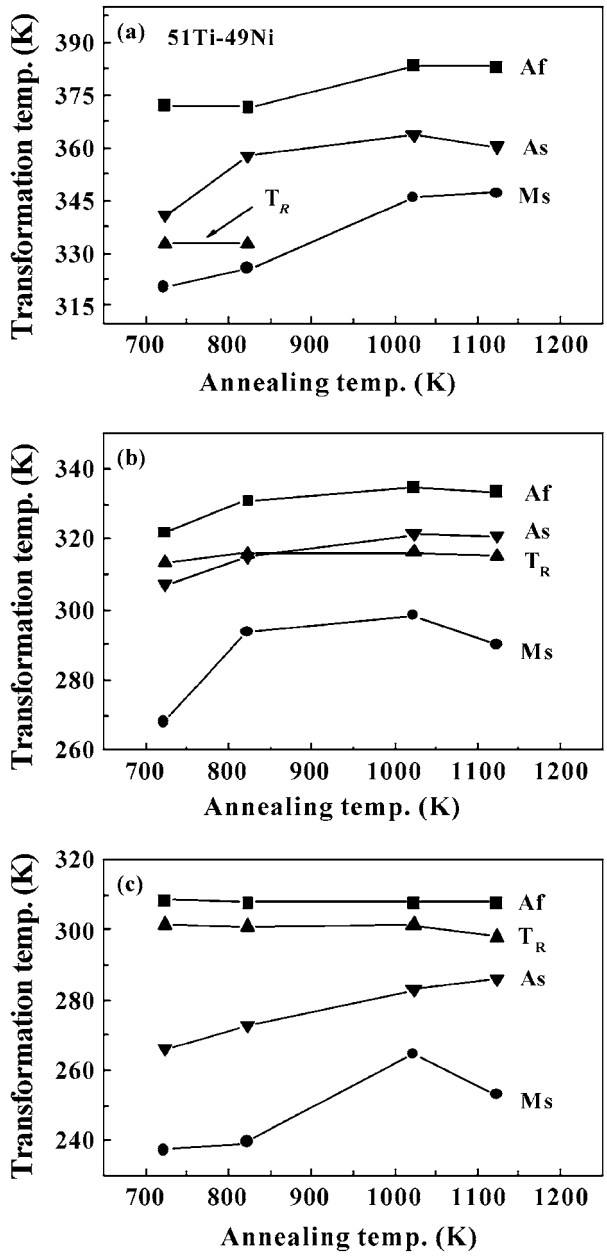

Figure 9 The relationship between transformation temperatures and annealing temperatures.

51Ti-48.5Ni-0.5Mo alloys, while they are separated in the 51Ti-48.3Ni-0.7Mo alloy.

As mentioned previously, for medical applications of Ti-Ni based shape memory alloys, they should be deformed to wire. Since strain hardening exponent of Ti-Ni based shape memory alloys is very high, intermediate annealing during wire drawing process is necessary. Af of the binary Ti-Ni alloy change during deformation and intermediate annealing process as seen in Fig. 9. In order to apply binary Ti-Ni shape memory alloys to medical field, very precise control of the amount of deformation and intermediate annealing condition should be done, since Af of the alloys is sensitive to the amount of cold working, annealing temperature and annealing time. As seen in the Fig. 9, however, Af of the 51Ti-48.3Ni-0.7Mo alloy does not depend on the conditions of intermediate annealing treatment. Therefore, it is concluded that the a 51Ti-48.3Ni-0.7Mo alloy is very suitable for medical applications.

3.2. Wire drawing characteristics of Ti-Ni-Mo alloys

In order to investigate general deformation characteristics of Ti-Ni binary and Ti-Ni-Mo ternary alloys, tensile tests were made at room temperature, and then typical stress vs. strain curves obtained are shown in Fig. 10. All specimens were cold drawn by 25%, and then annealed at 823 K for 0.6 ks. At room temperature, the Ti-Ni binary alloy is transformed into the B19′ martensite completely before loading as seen in Fig. 5 and so the plateau region in the stress vs. strain curve corresponds to a rearrangement of the B19′ martensite variants. In the 0.5at%Mo alloy, only the R phase exists before loading as seen in Figs 6 and 8 and so the plateau region in the curve corresponds to the stress induced R-B19′ transformation. In the 0.7at%Mo alloy, a deflection (designated by an arrow) appears, and the plateau region appears at higher stress level. Since the B2 parent phase and the R phase coexists before loading, the deflection is ascribed to a rearrangement of variants of the R phase and the stress-induced B2-R transformation, and the plateau region is ascribed to the stress induced R-B19′ transformation.

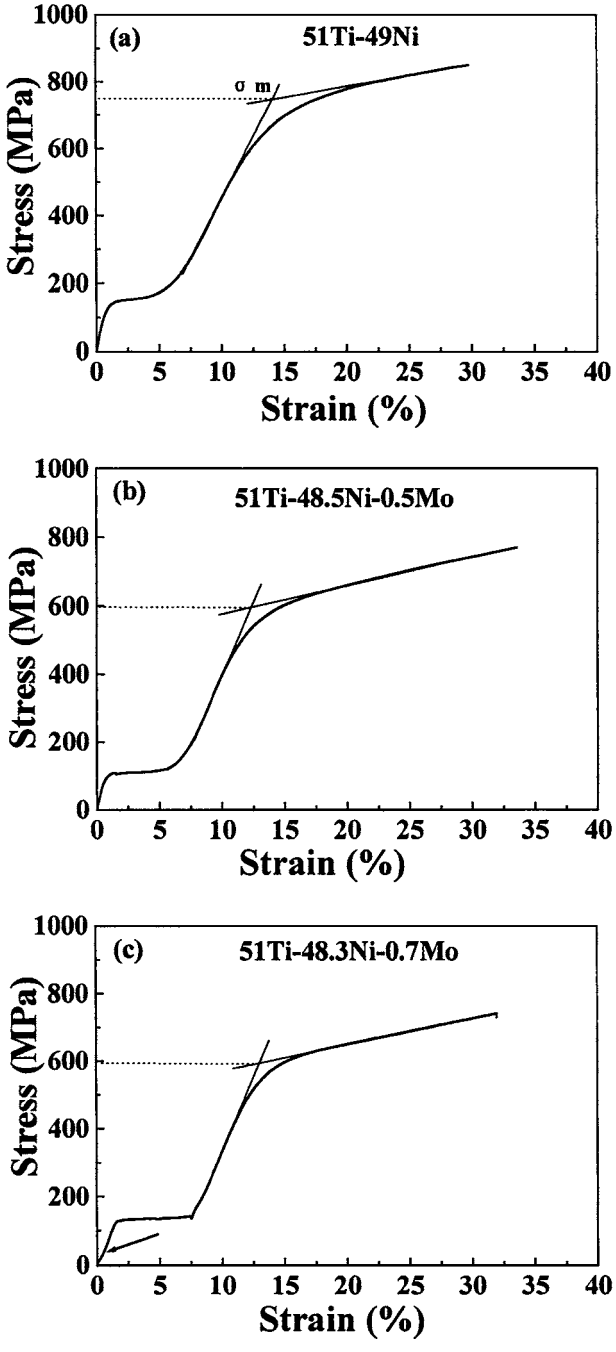

Figure 10 Stress-strain curves of the thermo-mechanically treated (a) 51Ti-49Ni, (b) 51Ti-48.5Ni-0.5Mo and (c) 51Ti-48.3Ni-0.7Mo alloys.

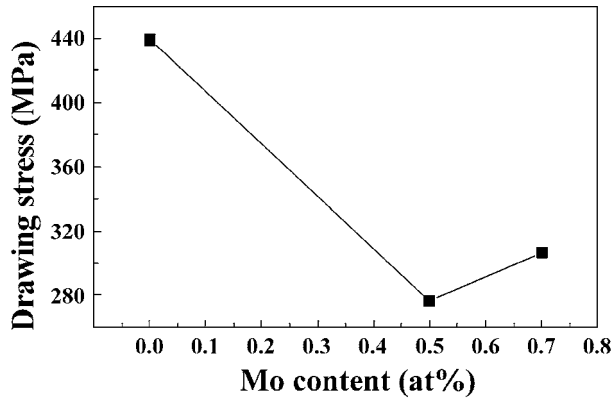

Figure 11 Drawing stress at Ms temperature.

On increasing applied stress over the stress corresponding to the plateau, the thermally and/or stress induced B19′ martensite is deformed elastically, and then the macroscopic plastic deformation starts to occur at the stress of σm. While wire drawing being done, large amounts of plastic deformation by slip occurs. In the above mentioned three alloys, during being drawn at room temperature, slip deformation should occur by a plastic deformation of the B19′ martensite. Examining stress vs. strain curves in Fig. 10, it is found that σm of the Ti-Ni-Mo alloys is lower than σm of the Ti-Ni binary alloy. From the result, it is expected that the stress (σd) required for wire drawing of the Ti-Ni-Mo alloys is lower than that of the Ti-Ni binary alloy. Fig. 11 shows σd of the Ti-Ni and Ti-Ni-Mo alloys, which are measured at Ms. It is clear that σd of the Ti-Ni alloy is larger than that of Ti-Ni-Mo alloys. Therefore, it is concluded that drawability of a Ti-Ni alloy is improved largely by Mo addition.

As mentioned previously, since strain hardening exponent of Ti-Ni based alloys is very large, intermediate annealing process to release internal stress introduced by cold drawing is necessary during wire drawing. The residual internal stress after the intermediate annealing process depends on the amount of cold working and annealing temperature, and it affect subsequent cold working. Fig. 12 shows a relationship between σd and the amount of cold working. As seen in the figure, σd increases with increasing cold working. This is because the residual internal stress which hinders workability increases with increasing cold working. Fig. 13 shows annealing temperature dependence of σd. σd is seen to decrease with raising annealing temperature. From Figs 12 and 13, we can conclude tentatively that an high temperature annealing above 823 K after small amount of cold drawing is desirable for a good drawability.

When the intermediate annealing is made in air, an oxidation on the surface of Ti-Ni alloys occurs. It was

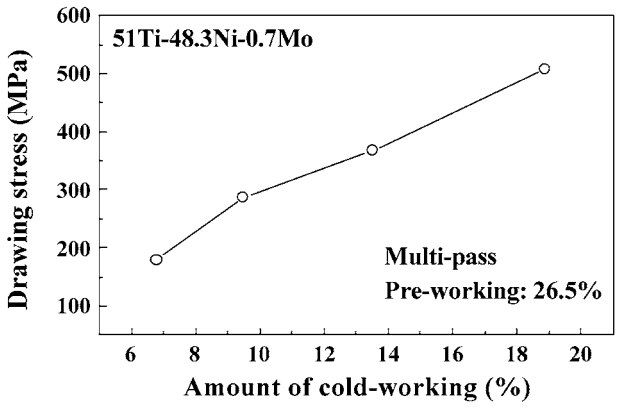

Figure 12 The relationship between σ d and the amount of cold working.

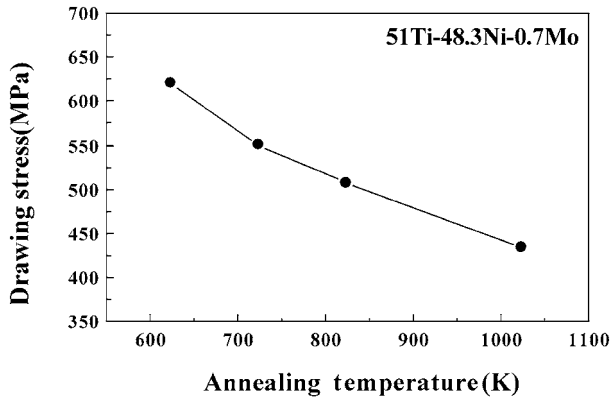

Figure 13 The relationship between drawing stress and annealing temperatures.

reported that an oxide film on Ti-Ni alloys is detrimental to their shape memory effect and pseudoelasticity [6]. Oxidation behaviors depends on annealing temperature and time [13]. Therefore it is necessary to investigate oxidation behaviors of Ti-Ni-Mo alloys for determining an optimum wiredrawing condition. Morphology of surfaces of the 51Ti-48.3Ni-0.7Mo alloy obtained by scanning electron microscopy are shown in Fig. 14. Fig. 14a is a micrograph of the surface of the alloy wire annealed at 823 K for 0.6 ks. The surface of the alloy wire is found to be covered by dense oxide film. After being annealed, the alloy was drawn by 20% at room temperature. Fig. 14b is a micrograph obtained after the cold drawing. It should be noted here that most of the oxide film formed during annealing process is removed by cold drawing. The lines aligned along vertical direction (drawing direction) in the figure are scratches formed on the surface of the alloy wire during cold drawing. Fig. 14c is a micrograph of the alloy annealed at 1023 K for 0.6 ks. An porous oxide film is seemed to cover all the surface of the alloy. As can be seen in Fig. 14d, the porous oxide film is removed by cold drawing. Fig. 15 shows SEM micrographs of the cross section of the alloy wire annealed at 1023 K for 3.6 ks. As can be seen in Fig. 15a, two kinds of oxide layer, that is, the outer layer with thickness of about 7 μm and the inner layer with thickness of about 1 μm are found to be formed. From X-ray diffraction and energy dispersive X-ray analyses, it was found that the outer layer is mainly TiO_2 and that the inner layer is a mixture

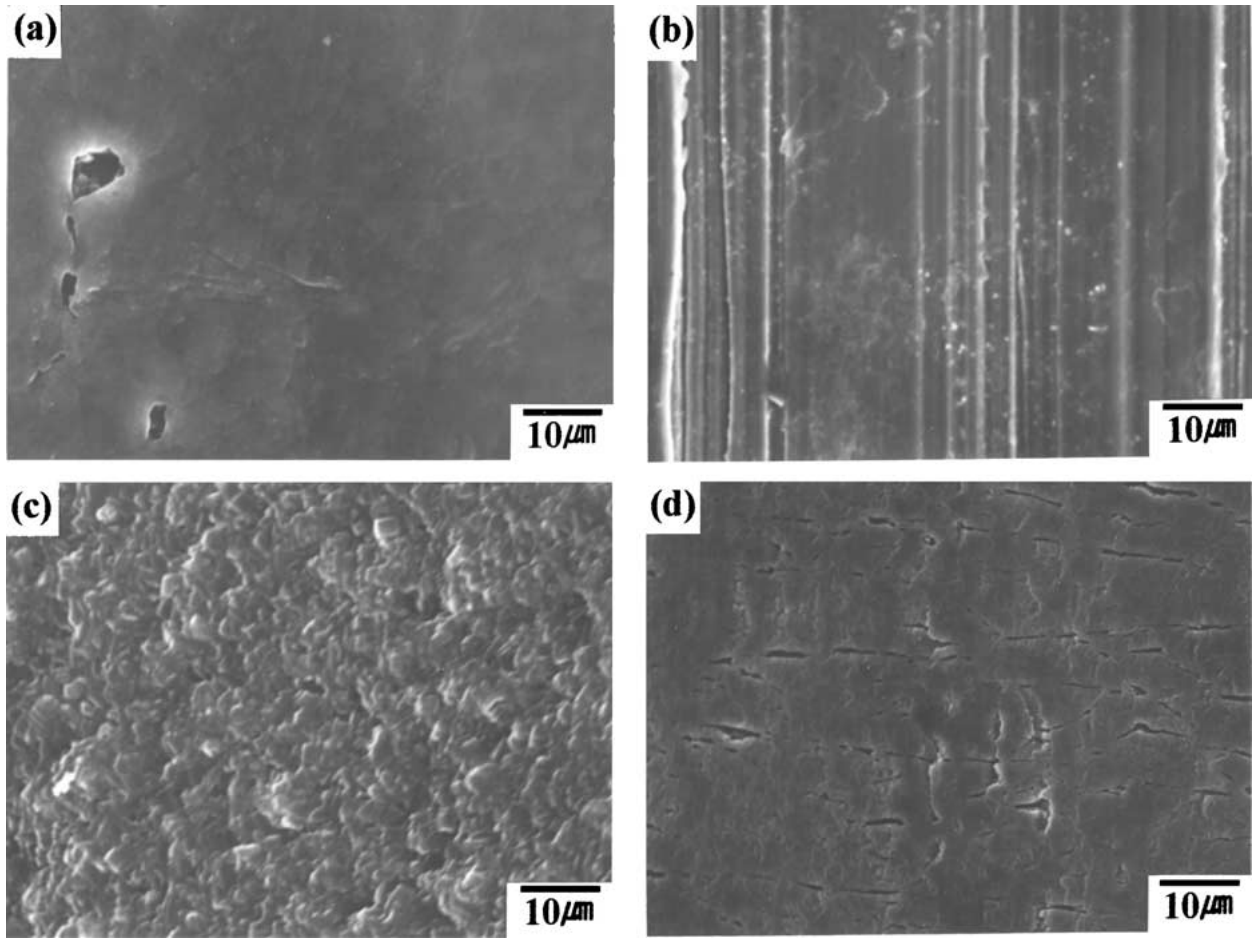

Figure 14 (a) and (c) are SEM micrographs of specimens annealed at 823 K and 1023 K, respectively. (b) and (d) are SEM micrographs obtained after cold drawing (a) and (c), respectively.

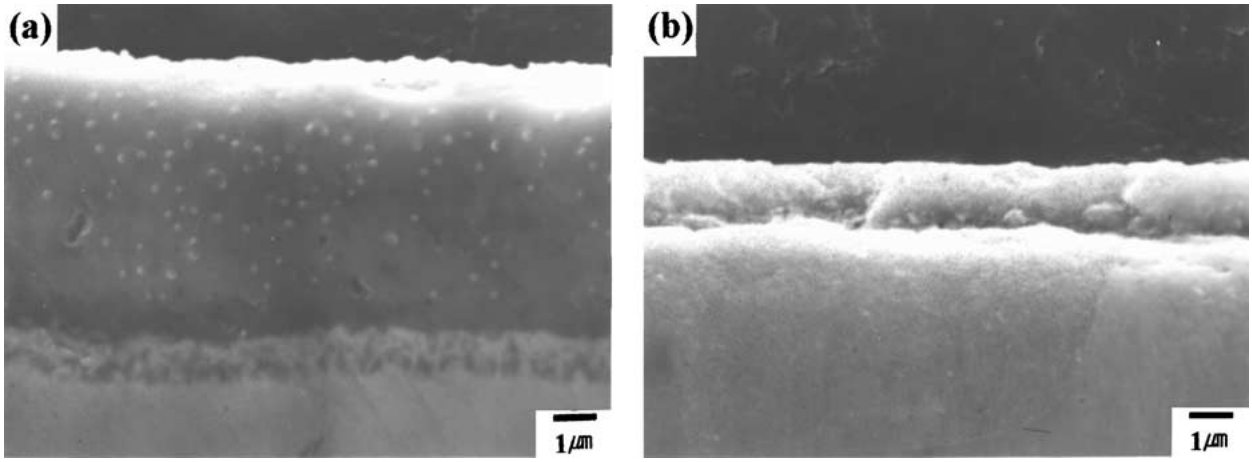

Figure 15 SEM micrographs of the cross section of the 51Ti-48.3Ni-0.7Mo alloy wire. (a) before wire drawing, (b) after wire drawing.

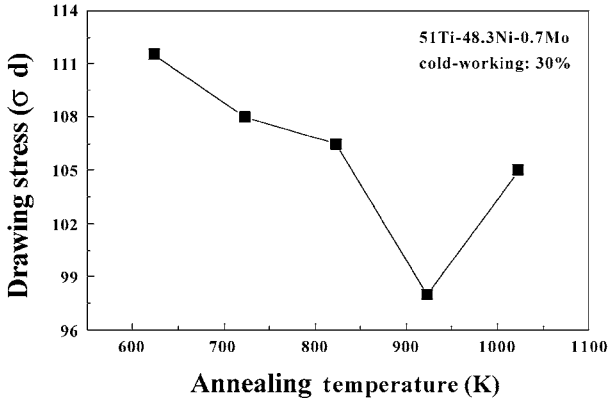

Figure 16 The relationship between drawing stress and annealing temperatures.

of TiO_2, pure Ni and Ti_3Ni_4 [14]. After wire drawing, the outer oxide film is removed as seen in Fig. 14b, and the inner layer remains, although some microcracks are seen as seen in Fig. 14d. That is, the dense oxide film made by annealing at 823 K is removed, while that made by annealing at 1023 K is not removed by cold drawing.

In order to investigate the effect of oxide films on $\sigma\, d$, specimens were annealed at 623 K–1023 K for 3.6 ks in air, and then drawn by 30% with measuring $\sigma\, d$. Results obtained are shown in Fig. 16. As seen in the figure, $\sigma\, d$ decreases with raising annealing temperature up to 923 K. This is attributed to the fact that the residual internal stress which hinders workability decreases with raising annealing temperature. However, $\sigma\, d$ increases when the annealing temperature is above 923 K with raising annealing temperature. This may be ascribed to a formation of the oxide films. As mentioned previously, during wire drawing the specimen after being annealed at 1023 K, the thick outer oxide film is removed, but the inner oxide film remains. The inner layer may not be deformed during wire drawing, and consequently increases $\sigma\, d$. In contrast to Fig. 16, $\sigma\, d$ decreased monotonously with raising annealing temperature when annealing was made in vacuum as seen in Fig. 13.

In order to determine the optimum wire drawing condition of Ti-Ni-Mo shape memory alloys for medical application, transformation temperature, drawability should be considered simultaneously. As mentioned before, Af of a 51Ti-48.3Ni-0.7Mo alloy is near temperature of human body and it dose not depend on the intermediate annealing condition. However, drawability decreases with increasing intermediate annealing temperature when intermediate annealing treatments are made at the temperature above 923 K in air, since a thick oxide film which is detrimental to drawability is formed. Therefore, it is concluded that the optimum intermediate annealing temperature for wire drawing of a 51Ti-48.3Ni-0.7Mo alloy is 823 K.

4. Conclusions

1) Substitution of Mo for Ni of a 51Ti-49Ni(at%) alloy induced the B2-R transformation, and consequently it transformed in two stages, i.e., from the B2 to the R, and then from the R to the B19′. The stability of the R phase increased with increasing Mo content.

2) In the thermo-mechanically treated 51Ti-48.3Ni-0.7Mo(at%) alloy, reverse transformation temperature, Af, kept constant, irrespective of thermo-mechanical treatment conditions, while it changed largely in the thermo-mechanically treated 51Ti-49Ni(at%) and 51Ti-48.5Ni-0.5Mo(at%) alloys.

3) Drawing stress of 51Ti-48.3Ni-0.7Mo(at%) ternary alloys was smaller than that of a 51Ti-49Ni(at%) binary alloy. This means that drawability of a Ti-Ni binary alloy is improved by Mo addition.

4) Drawing stress of 51Ti-48.3Ni-0.7Mo(at%) ternary alloys decreased monotonously with raising intermediate annealing temperature when intermediate annealing treatments were made in vacuum. However, it decreased below 923 K, and then increased above 923 K with raising intermediate annealing temperature when intermediate annealing treatments were made in air. This was ascribed to a formation of thick oxide film.

References

1. S. MIYAZAKI, K. OTSUKA and Y. SUZUKI, *Scripta Metall.* **15** (1987) 287.
2. S. MIYAZAKI and K. OTSUKA, *Metal. Trans.* **17A** (1986) 53.
3. T. SABURI, S. NENNO, Y. NISHIMOTO and M. ZENIYA, *Tetsu to Hagane* **72** (1986) 571.

4. T. TODOROKI and H. TAMURA, *Mat. Trans., JIM* **28** (1987) 83.
5. S. MIYAZAKI and K. OTSUKA, *Phil. Mag.* **50A** (1984) 393.
6. H. C. LIN, S. K. WU and Y. C. YEN, in Proceedings of the 2nd Pacific Rim International Conference on Advanced Materials and Processing, Kyongju, June 1995, edited by K. S. Shin *et al*. (The Korean Institute of Metals and Materials, 1995) p. 1167.
7. V. E. GUNTER, "Medical Materials and Implants with Shape Memory Effect" (Tomck, 1998) p. 180.
8. I. P. LIPSCOMB and L. M. D. NOKES, "The Application of Shape Memory Alloy in Medicine" (Paston Press Ltd, London, 1996) p. 5.
9. C. M. HWANG, M. E. MEICHLE, M. B. SALAMON and C. M. WAYMAN, *Phil. Mag.* **47A** (1983) 31.
10. M. B. SALAMON, M. E. MEICHLE and C. M. WAYMAN, *Phys. Rev. B* **31** (1985) 7306.
11. C. M. HWANG and C. M. WAYMAN, *Scripta Metall.* **17** (1983) 381.
12. T. H. NAM, D. W. CHUNG, J. P. ROH, H. W. LEE and S. G. HUR, *Scr. Metall. et Mater.*, Submitted.
13. C. L. CHU, S. K. WU and Y. C. YEN, *Mat. Sci. & Eng.* **A126** (1996) 193.
14. T. H. NAM, unpublished work.

Received 29 June 2000
and accepted 21 March 2001